Pd/WO$_3$-ZrO$_2$ Catalysts: Synthesis, Characterization and Catalytic Evaluation

L.F. Chen[*,a], S.P. Ramirez Sebastian[**,a], J.A. Wang[***,a] and J.L. Contreras[****,b]

[a] Superior School of Chemical Engineering and Extractive Industries, National Polytechnic Institute, Av. Politécnico, S/N, Col. Zacatenco, 07738, Mexico City, Mexico
[b] Departamento de Ciencias Básicas, Universidad Autónoma Metropolitana-A, Av. San Pablo No. 180, 02200 México City, Mexico
[*]chenlf2001@yahoo.com; [**]silvia_patricia_rs@hotmail.com; [***]jwang@ipn.mx; [****]jlcl@coreo.azc.uam.mx

ABSTRACT

Several 1 wt% Pd/WO$_3$-ZrO$_2$ catalysts were prepared using a sol-gel technique by varying WO$_3$ content in 5, 10, 15 and 25 wt%. The crystalline structure, acidity, reducibility and morphologies were studied by XRD, FTIR, H$_2$-TPR, STEM and Raman spectroscopic techniques. XRD analysis shows that the support oxides chiefly contain tetragonal zirconia together with WO$_3$ phase on surface. With Raman spectroscopy, the surface structure of WO$_3$ (800 cm^{-1} for W-O bond, 268 cm^{-1} for W-O-W bonds, and 711 cm^{-1} for W=O bond) are observed. *In situ* FTIR spectra confirm that both Lewis and Brønsted acid sites are present in the catalysts. In the hydroisomerization of n-heptane, the highest n-heptane conversion (60.8%) is obtained over 1 wt% Pd/WO$_3$-ZrO$_2$ with 25 wt% WO$_3$ at 300 °C and the isomerization selectivity reaches 90%. Among the multibranched isomers, 2,3- dimethylpentane is the main component.

Keywords: n-heptane, hydroisomerization, Pd/WO$_3$-ZrO$_2$, catalysts, sol-gel.

1 INTRODUCTION

The hydroisomerization of hydrocarbons is a full green chemistry process, by which the n-alkanes with straight carbon chain are transformed into branched isomers that are used to boost the research octane number (RON) of the gasoline fuel. For example, the RON of n-heptane is 0, it rises up to 56, 92 and 120 for 3-methylhexane, 2, 3-dimethylpentane and toluene, respectively [1]. The isomerization processes of n-C$_5$ and n-C$_6$ have been commercialized; however, to date, n-heptane isomerization is still in laboratory stage. The current industrial catalysts for C$_5$/C$_6$ isomerization like Pt/mordenite are not suitable for n-heptane isomerization, because of strong diffusion limitation to the multibranched isoheptanes in the small pores of mordenite [2]. It is reported that the tungstated zirconia catalysts exhibit good isomerization activity of hydrocarbons where the strong acidity takes a key role [3-5]. However, other researchers claim that the catalytic activity is independent of the acidity of tungstated zirconia but is related to the redox properties of WO$_3$ or the formation of W^{5+} species [6, 7]. In fact, the catalytic properties of the tungstated zirconia catalysts are closely related to synthetic techniques [8]. The present work aims at searching for new Pd/WO$_3$-ZrO$_2$ catalysts prepared with a sol-gel method for n-heptane isomerization. Synthesis, characterization and catalytic evaluation of a series of Pd/WO$_3$-ZrO$_2$ catalysts are reported.

2 EXPERIMENTAL

2.1 Support and Catalysts Preparation

Four WO$_3$-ZrO$_2$ oxides were prepared by a sol-gel technique using (NH$_4$)$_6$W$_{12}$O$_{39}$·H$_2$O as WO$_3$ precursor and Zr[O(CH$_2$)$_3$CH$_3$]$_4$ as ZrO$_2$ precursor. The WO$_3$ content varied from 5 wt% to 10, 15 and 25 wt%. These oxides are noted as 5WZ, 10WZ, 15WZ and 25WZ. In the preparation, 100 ml of isopropanol was used as solvent, then a solution was prepared by dissolving a desired ammont of (NH$_4$)$_6$W$_{12}$O$_{39}$·H$_2$O and Zr[O(CH$_2$)$_3$CH$_3$]$_4$ with 37% HNO$_3$. This mixing solution was added, drop by drop, into the isopropanol solution with vigorous agitation for 40 min. Gel was formed at room temperature during the addition. Afterword, the precipitate was filtered and dried by evaporating the solvent using an evaporator at 80 °C. The dried material was calcined at 800 °C in air for 3 h. The 1 wt%Pd/WO$_3$-ZrO$_2$ catalysts were prepared by impregnating PdCl$_2$ aqueous solution on the support, followed by the steps of drying at 80 °C for 12 h and calcination at 450 °C for 3 h. These catalysts are noted as Pd/5WZ, Pd/10WZ, Pd/15WZ and Pd/25WZ.

2.2 Catalysts Characterization

X-ray diffraction analysis was performed on a Siemens Diffractometer Model D-5000, using Co-Kα (λ = 1.789 Å) radiation at 40 kV and 35 mA. The diffraction patterns were recorded at 2θ range between 10 and 60 ° with a step of 0.02 ° and a measure time 2s each step. The phase component determination was checked with the data base of the Joint Committee on Powder Diffraction Standards (JCPDS).

Temperature-programmed reduction (TPR) of the samples was performed using 10% H_2-90% He flow (50 cm^3min^{-1}) with a TPD/TPR-2900 analyzer (Micromeritics). 50 mg catalyst were placed on a U-type glass reactor and the temperature was raised from room temperature to 1000 °C at a heating rate of 10 °C/min. Water and other products formed in TPR were detected with a thermal conductivity detector operating in a continuous mode.

The surface morphology and particle size distribution were analyzed using scanning transmission electron microscopy STEM (JEM-2200FS). The experiments were carried out with accelerating voltage of 200 kV.

The surface species of the catalysts were analyzed using Raman spectroscopic method. The Raman spectrum was obtained at room temperature using a LabRam HR 800 spectrometer. A laser diode of He-Ne system supplies a 633 nm exciting line and spectral resolution was 4 cm^{-1}.

The surface acidity of the catalysts was measured using pyridine adsorption of Fourier-transform infrared (FTIR) technique on a 170-SX spectrometer. Before pyridine adsorption, each sample was heated to 300 °C for 60 min under vacuum, in order to eliminate the adsorbed water or impurities on the surface; and then it was cooled to room temperature. Afterward, the solid wafer was exposed to pyridine, by breaking inside the spectrometer cell, a capillary containing 50 μl of liquid pyridine. The IR spectra were recorded at various conditions by increasing the IR cell temperature from 25 to 400 °C. The quantitative calculation of Lewis and Brønsted acid sites was made with respect to the area of the adsorption bands at 1450 cm^{-1} and 1540 cm^{-1}, respectively.

2.3 Catalytic Evaluation

The n-heptane isomerization reactions were carried out in a down-flow fixed-bed reactor (i.d. = 1 cm, 20 cm in length) in the presence of hydrogen at atmospheric condition. 50 mg catalyst were loaded in reactor and the H_2/n-heptane molar ratio was 5.6. The liquid n-heptane was placed in a glass saturator with a water bath to control the temperature. Hydrogen (99.9%) passed through it at a flow rate of 30 ml/min and brought the n-heptane feed into the reactor. The reaction temperature varied from 200 to 400 °C with a programmed temperature control system XMTG-9000 at a heating rate of 5 °C/min. Before the reaction, palladium oxide on the catalysts was reduced with hydrogen for 2 h at 300 °C. The products were analyzed using an on-line analytical system (GC Varian3300) equipped with a flame ionization detector (FID) and a HP-PONA 50 m×0.2 mm capillary column maintained at 30 °C.

In the n-heptane isomerization reactions, the experimental data were recorded after the analysis and reaction system were stable. The catalytic activity was expressed as n-heptane conversion and the isomerization selectivity is noted as the sum of all the isoheptanes relative to all the products.

3 RESULTS AND DISCUSSION

Figure 1 shows the XRD patterns of the four WO_3-ZrO_2 samples. The oxides chiefly contain tetragonal zirconia and minor monoclinic ZrO_2 together with WO_3 phase. The peaks at 2θ = 30, 35, 50° correspond to crystalline structures of tetragonal zirconia. Some peaks with low intensity at 2θ =24, 28, 33, 40, 45, 51, and 55° indicate the formation of small amount of monoclinic zirconia phase [9, 10]. Several groups of XRD peaks at 2θ =26, 28, 32, 50, 52, and 54° are related to WO_3 phase.
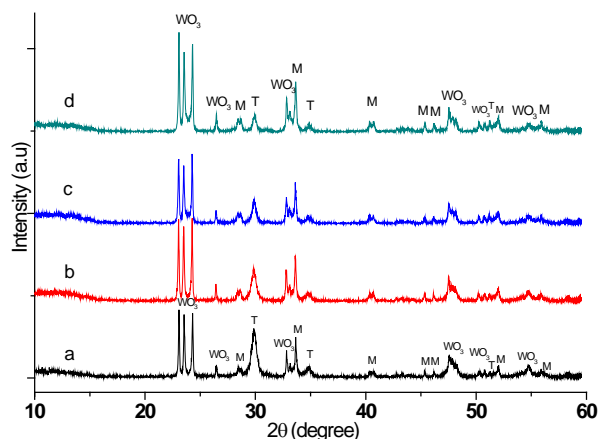

Figure 1. XRD patterns of WO_3-ZrO_2 oxides. a:5wt% WO_3; b:10wt% WO_3; c:15wt% WO_3; d:25wt% WO_3.
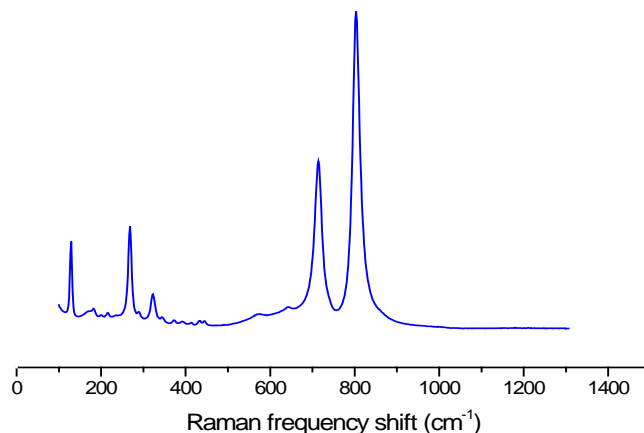

Figure 2. A Raman spectrum of the 1%Pd/5%WZ

With Raman spectroscopy, the surface structure of WO_3 (800 cm^{-1} for W-O bond, 268 cm^{-1} for W-O-W bonds, and 711 cm^{-1} for W=O bond) were observed (Figure 2). With repect to ZrO_2, the bands corresponding to the tetragonal metaestable ZrO_2 were observed at 148 cm^{-1}, 275 cm^{-1}, 323 cm^{-1}, 455 cm^{-1} and 648 cm^{-1} [11]. While the monoclinic ZrO_2 shows several weak bands at 167 cm^{-1},179 cm^{-1}, 220 cm^{-1}, 380 cm^{-1} and 472 cm^{-1}, respectively [12].

The intensity of the bands related to WO_3 phases are much stronger in comparison with that of the ZrO_2, which seems to indictate that most of the WOx phases are dispersed on the surface of the ZrO_2 phase.

The surface feature and morphologies of the catalysts were also investigated by STEM. Figure 3 shows the STEM micrograph of the 1 wt%Pd/15%WO_3-ZrO_2. All the elements Zr, W, Pd and O are clearly present in the sample as shown in EDS spectrum, Figure 4. It is interesting to observe that most of WO_3 are dispersed on the surface of the ZrO_2 crystals, which is in good agreement with the results obtained from Raman spectrum. During the calcination process of the samples, WO_3 tried to segragate from the mixed oxides, enriching in the surface and interface of the ZrO_2 phases.
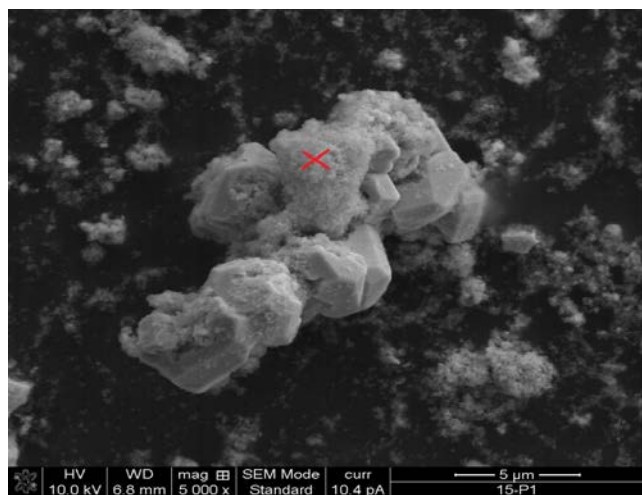

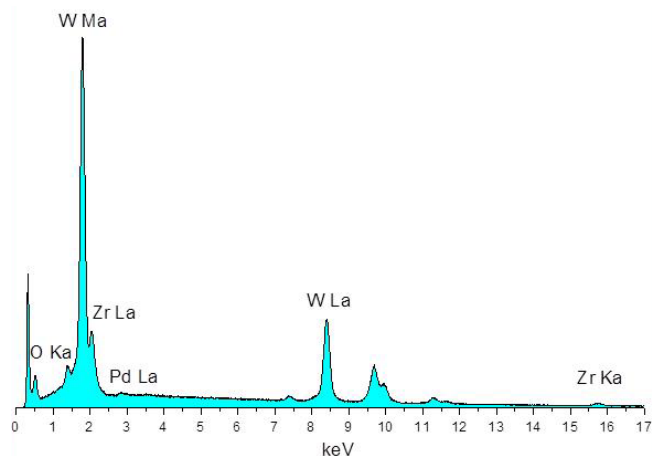Figure 3. A STEM micrograph of the 1%Pd/15%WZ sample.

Figure 4. A EDS spectrum of the point with red cross marked on 1%Pd/15%WZ sample.

The reducibility of the PdO/WO_3-ZrO_2 samples were studied by H_2-TPR. Figure 5 shows that PdO can be reduced at low temperature, i.e. below 100 °C. It is noted that a small negative peak appears in TPR profiles at approximately 90°C, which indicates the release of hydrogen. This phenomenon can be explaned by assuming that during the reduction of PdO particles, a new metaestable phase β-PdH_x was formed [13]. It was unstable and was decomposed around 95 °C to release hydrogen. These reduction precedures can be expressed by the following reactions:

$$PdO + H_2 \rightarrow Pd + H_2O \tag{1}$$
$$0.5xH_2 + Pd \rightarrow \beta - PdHx \tag{2}$$
$$\beta - PdHx \rightarrow Pd + 0.5xH_2 \tag{3}$$

In the TPR profiles, there are two strong peaks between 550 °C and 900 °C, whose peak areas vary with the WO_3 content in the samples. It is observed that in the sample with 5 wt% of WO_3, the area of the peak around 670 °C is greater than the peak at 800 °C; however, as the WO_3 content increases, the area of the higher temperature peak gradually increases and finally, it is greater than that of the lower temperature peak, as shown in the sample with 25 wt% of WO_3. It is reported that the peak in TPR profile between 300-500 °C corresponds to the reduction of WO_3 to $WO_{2.9}$; the one between 550 and 750 °C corresponds to the reduction of $WO_{2.9}$ to WO_2, and the one between 750 and 950 °C to the reduction step of $WO_2 \rightarrow W$ [14].
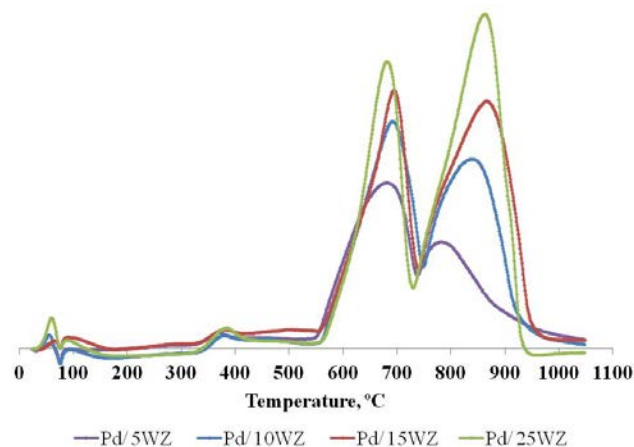

Figure 5. H_2-TPR profiles of the PdO/ZrO_2-WO_3

The surface acidity of the catalysts was determined by in situ FTIR spectroscopy of pyridine adsorption technique. FTIR spectra confirm that both Lewis and Brønsted acid sites are present in the catalysts surface as indicated by the pyridine adsorption bands at 1450, 1580 and 1595 cm^{-1}. Most of the Lewis and Brønsted acidity remain on the catalysts above 300 °C.

In the hydroisomerization of n-heptane, the highest n-heptane conversion (60.8%) was obtained over 1 wt% Pd/WO_3-ZrO_2 with 25 wt% WO_3 at 300 °C and the isomerization selectivity was around 90%. In low reaction temperature, i.e., 280 °C, the isomerization selectivity was

100 %. As reaction temperature increased, the selectivity decreased due to cracking, Figure 6.

In the products dsitribution, various C_7 isomers, like 2-methylhexane, 3-methylhexane, 2,2-dimethylpentane, 2,3-dimethylpentane, 2,4-dimethylpentane, and 3,3-dimethylpentane were detected. Their yields were dependent of the reaction temperature and varied with WO_3 concentration. In the monobranched isomers, 2-methylhexane was dominant; while, in the multibranched isomers, 2,3- dimethylpentane was the main component, which has high RON. The products distribution indicates that it is possible to use our sol-gel Pd/WO_3-ZrO_2 catalysts for obtaining n-heptane isomers with high octane number.
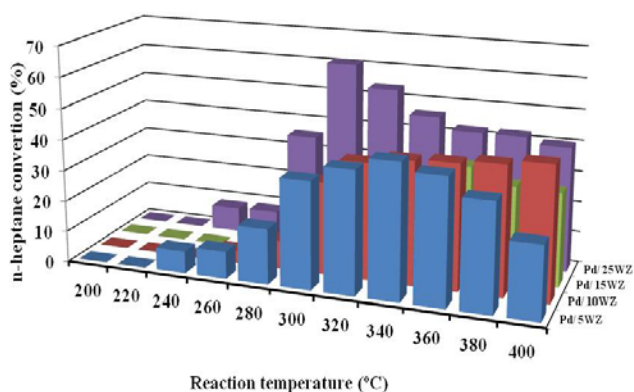

Figure 6. n-heptane conversion as a function of reaction temperature over various catalysts.

4 CONCLUSIONS

In the sol-gel WO_3-ZrO_2 mixed oxides, tetrogonal ZrO_2 is the main phase and WO_3 are enriched on the surface of ZrO_2 or in the interface of the oxides. During the TPR procedure, PdO is easily reduced below 100 °C and a new metaestable phase β-PdH_x is formed, which is unstable and is decomposed around 95 °C to release hydrogen. WO_3 oxide can be reduced by three steps at different temperatures. The Pd/WO_3-ZrO_2 catalysts contain both Lewis and Brønsted acid sites. In the hydroisomerization of n-heptane, the highest n-heptane conversion (60.8%) is obtained over 1 wt% Pd/WO_3-ZrO_2 with 25 wt% WO_3 at 300 °C with isomerization selectivity around 90%. In the monobranched isomers, 2-methylhexane is dominant; while, in the multibranched isomers, 2,3- dimethylpentane is the main component.

REFERENCES

[1] J.A.Wang, X.L. Zhou, L.F. Chen, L.E. Noreña, G.X. Yu, C.L. Li, Journal of Molecular Catalysis A: Chemical 299, 68–76, 2009.

[2] V.M. Akhnedov, S.H. Al-Khowaiter, J.K. Al-Refai, Appl. Catal. A: General 252, 353-361, 2003.

[3] Y.Q. Song, C.L. Kang, Y.L. Feng, F. Liu, J.A. Wang, L.Y. Xu, Catal. Today 148, 63-69, 2009.

[4] C.C. Hwang, X.R. Chen, S.T. Wong, C.L. Chen, C.Y. Mou, Appl. Catal. A. 323, 9-17, 2007.

[5] S.T. Wong, T. Li, S. Cheng, J.F. Lee, C.Y. Mou, J. Catal. 215, 45-56, 2003.

[6] M.A. Cortés-Jácome, C. Angeles-Chavez, E. López-Salinas, J. Navarrete, P. Toribio, J.A. Toledo, Appl. Catal. A. 318, 178-189, 2007.

[7] S.Kuba, P. Lukinskas, R.Ahmad, F.C. Jentoft, R.K. Grasselli, B.C. Gates, H. Knözinger, J. Catal. 219, 376-388, 2003.

[8] S. D. Rossi, G.Ferraris, M. Valigi, D. Gazzoli, Appl. Catal. A. 231, 173-184, 2002.

[9] M. A. Cortés-Jácome, J. A. Toledo-Antonio. A. Hernández, and X. Bokhimiz. Journal of Solid State Chemistry 164, 339–344, 2002.

[10] M. Signoretto, M. Scarpa, F. Pinna, G. Strukul, P. Canton, A. Benedetti. Journal of Non-Crystalline Solids 225,178–183, 1998.

[11] A.-S. Mamede, E. Payen, P. Grange, G. Poncelet, A. Ion, M. Alifanti, V.I. Pârvulescu. J. Catalysis, 223,1-12, 2004.

[12] S.R. Vaudagna, R.A. Comelli, N.S. Fígoli. Applied Catalysis A: General 164, 265-289, 1997.

[13] L.F. Chen, J.A. Wang, M.A. Valenzuela, X. Bokhimi, D.R. Acosta, O. Novaro. Journal of Alloys and Compounds 417 (2006), pp. 220-223.

[14] D.G. Barton, S. Soled, G. Meitzner, G.A. Fuentes, E. Iglesia. J. Catal. 181, 57-72, 1999.